Feasibility of NIR interactance hyperspectral imaging for on-line measurement of crude composition in vacuum packed dry-cured ham slices.

Gou, P.[1*], Santos-Garcés, E.[1], Høy, M.[2], Wold, J.P.[2], Liland, K.H.[2] & Fulladosa, E.[1]

[1]IRTA. XaRTA. Food Technology. Finca Camps i Armet, E-17121 Monells (Girona), Spain
[2]Nofima Mat AS, Osloveien 1, N-1430 Ås, Norway
[*]Corresponding author: Pere Gou
E-mail: pere.gou@irta.cat; Tel.: +34 972 630 052; Fax: +34 972 630 373

Abstract

There is a growing market for packaged slices of dry-cured ham. The heterogeneity of the composition of slices between packages is an important drawback when aiming to offer consumers a product with a known and constant composition which fits individual consumer expectations. The aim of this work was to test the feasibility of NIR interactance imaging for on-line analysis of water, fat and salt and their spatial distribution in dry-cured ham slices. PLSR models for predicting water, fat and salt contents with NIR spectra were developed with a calibration set of samples (n = 82). The models were validated with an external validation set (n = 42). The predictive models were accurate enough for screening purposes. The errors of prediction were 1.34%, 1.36% and 0.71% for water, fat and salt, respectively. The spatial distribution of these components within the slice was also obtained.

Keywords: NIR interactance; hyperspectral imaging; on-line prediction; chemical composition; dry-cured ham

Highlights:

Composition of dry-cured ham is predicted with NIR interactance hyperspectral imaging.

Average spectra of packed slices of ham are used to build PLS prediction models.

Water, fat and salt predictions are accurate enough for on-line screening purposes.

Informative images of water, fat and salt distribution in ham slices are obtained.

1. Introduction

Dry-cured ham is a traditional meat product widely consumed in the Mediterranean area and has traditionally been commercialized as whole pieces. However, in recent years there has been an increase in the commercialization of vacuum-packed dry-cured ham slices. This product is characterized by having a highly heterogeneous composition which is caused by many factors. Fat content in ham is affected by gender, genetic origin and feeding regime (Blasco et al., 1994; Gou, Guerrero, & Arnau, 1995; Lebret, 2008). Salt content depends on the salt uptake and its distribution within the ham. Salt uptake has been proved to depend on some raw ham characteristics such as the size and shape of raw hams, meat pH and fat content (Costa-Corredor, Muñoz, Arnau, & Gou, 2010; Guerrero, Gou, Alonso, & Arnau, 1996) as well as on salting conditions and pre-salting treatments (Santos-Garcés, Muñoz, Gou, Sala, & Fulladosa, 2012; Garcia-Gil et al., 2011). Water content in dry-cured ham is controlled through the weight loss of the hams during drying. However, weight loss of the entire ham is related to the average water content and this relationship varies with the presence of other variable components (fat and salt).

Major efforts have been made to produce dry-cured hams with homogeneous composition by sorting the raw hams into homogeneous groups and then optimising the drying processes for each group. Nevertheless, there is still large within group variation. Another important source of variation in packed slices is that the slices can consist of different muscles, which differ in their water, fat and salt contents (Arnau, Guerrero, Casademont, & Gou, 1995; Boadas, Gou, Valero, & Arnau, 2001). A better control of salting and drying processes could reduce the heterogeneity in salt and water contents, but it would have no effect on the fat distribution.

There is a variation in consumer preferences of ham in terms of saltiness, intramuscular fat and dryness (Resano, Sanjuán, Cilla, Roncalés, & Albisu, 2010; Hersleth, Lengard, Verbeke, Guerrero & Næs, 2011). The inclusion of this compositional information on the packages of sliced dry-cured ham would give consumers the possibility to choose the product according to their preferences. To obtain this information is therefore an important challenge for the industry. To achieve this objective, rapid and non-destructive on-line measurements of composition are needed.

Near-infrared (NIR) spectroscopy is a fast, non-destructive analytical technique which allows simultaneous assessment of numerous meat quality properties (Prieto, Roehe, Lavín, Batten, & Andrés, 2009). The NIR spectrum is characterized by overtones and combinations of the

fundamental molecular vibrations of molecules containing C-H, N-H and O-H groups (water, fat, protein, etc.). Salt does not absorb radiation in the NIR region, but it affects the molecular vibrations of the O-H groups and can therefore be estimated from the spectra (Ellekjaer, Hildrum, Naes, & Isaksson, 1993). Huang, Yu, Xu, and Ying (2008) reviewed the use of NIR spectroscopy for the on-line analysis of foods and beverages. Up to now, NIR technology has been dominated by reflectance instruments measuring one or more locations on the surface of the sample. On-line applications for meat products have traditionally been restricted to ground meat (Hildrum, Nilsen, Westard, & Wahlgren, 2004; Shackelford, Wheeler, & Koohmaraie, 2004). More recently NIR has also been applied to intact meat products. It has been used for estimating water and salt content at the surface of fermented sausages during the drying process (Collell, Gou, Arnau, Muñoz, & Comaposada, 2012), water and fat content of sliced sausages (Gaitán-Jurado, Ortiz-Somovilla, España-España, Pérez-Aparicio, & De Pedro-Sanz, 2008), and water and salt content at the surface of dry-cured ham during the resting and drying processes (Collell, Gou, Arnau, & Comaposada, 2011).

When measuring NIR in refleactance, the energy can penetrate several millimetres into the sample, but the measured signal will mainly represent the surface. Therefore, the usefulness of NIR reflectance instruments to estimate the average composition of a product depends on the homogeneity of the sample, or on how representative the sample surface is compared to the rest of the sample. NIR interactance instruments measure the light that is transmitted into the sample and then backscattered to the surface. Depending on the instrument set-up and on the sample, the penetration depth can be 10-15 mm, obtaining more representative measurements of the sample. Segtnan, Høy, Lundby, Narum, & Wold (2009) demonstrated that non-contact near infrared interactance hyperspectral imaging could be used for in-line fat distribution analysis in salmon fillets, which, as in dry-cured ham slices, have a heterogeneous distribution of fat both across the surface and in depth. Wold et al. (2006) used the same technology for on-line analysis of water content in salted and dried cod fish, which has a heterogeneous distribution of water. The method has also been reported to work well for on-line fat determination in batches of beef and pork trimmings (Wold, O'Farrell, Høy, & Tschudi, 2011; O'Farrel, Wold, Høy, Tschudi, & Schulerud, 2010).

The aim of this study was to test the feasibility of NIR interactance hyperspectral imaging for on-line analysis of water, fat and salt and their spatial distribution in dry-cured ham slices.

2. Materials and methods

2.1 Samples

Thirty seven dry-cured hams were purchased from six dry-cured ham producers that use raw hams with different characteristics as well as different salting/drying processes, to assure a wide range of fat, salt and water contents. The dry-cured hams were boned, pressed to fit into a parallelepiped shape (approximately 15 × 20 × 30 cm^3) and stored vacuum packed for three weeks. Thereafter, they were unpacked and a 2.5 cm thick slice perpendicular to the distal direction was sampled from all the hams. An additional slice was obtained from 13 hams out of the 37, and different regions of interest (ROIs) consisting of only one muscle (*Semimembranosus*, *Biceps femoris* or *Semitendinosus* muscles) were sampled. These ROIs were expected to be more homogeneous and to cover a wider range of composition in comparison to the whole slices. All samples were vacuum packed in bags (50 µm polyamide/100 µm polyethylene multilayer; water vapour permeability: 1.5 g / m^2 / 24 h; Sacoliva, S.L.®, Castellar del Vallès, Spain).

2.2 NIR analysis

Vacuum packed samples were scanned using a commercial on-line hyperspectral NIR imaging scanner, QMonitor (TOMRA Sorting Solutions, Asker, Norway), which combines non-contact NIR interactance measurements and spectral imaging (Wold et al., 2006). This scanner is made for industrial measurements over conveyor belts in the food industry and can handle belt speeds up to typically 1 m/s. The scanner was placed above a conveyor belt and the illuminating field was focused on the belt along a line perpendicular to the direction of movement (Figure 1). The light source consisted of 12 Reflecto halogen lamps of 50 W (BLV Licht- und Vakuumtechnik GmbH, Steinhöring, Germany). The light was transmitted into the sample and then back-scattered to the surface and then captured by the hyperspectral camera. The penetration depth of this system ranges from 15 mm to 20 mm, previously determined in dried salted cod (Wold et al., 2006). In the relatively dark and pigmented ham meat, the penetration is most likely closer to 15 mm than 20 mm. The field of spectral collection was parallel to the illuminating field about 2 cm further down. The backscattered light was focused on the CCD detector using a cylindrical lens. To minimise the collection of light reflected directly from the sample surface, a metal plate shield blocked the light between the

field of illumination and the field of detection. In the case of vacuum packed ham, it means that the signal contribution from the polyethylene film was minimised.

The scanner collected spectral images of 15 wavelengths/channels between 760 nm and 1040 nm with a spectral resolution of 20 nm. In this study, 12 wavelengths (from 820 to 1040 nm) were used. The output is an image of the sample of approximately 15 pixels in the direction perpendicular to belt movement × 400 pixels in the direction of belt movement. Each pixel consisted of a 12-wavelength spectrum. The system is calibrated by using a barium sulphate trough with a curved base. It is held under the separating wall, allowing light to pass from the field of illumination to the field of view.

The spatial resolution will vary with the speed of the conveyor belt. In this study the belt speed was about 0.4 m/s, resulting in a pixel size of 10 mm perpendicular to the belt movement direction and 0.5 mm in the belt movement direction. The concept of image resolution in this context is, however, slightly misleading, since the light collected in one defined measurement spot (pixel) has travelled from a much larger volume of the sample.

The individual intensity spectra (int) were subjected to log-transformation to obtain the absorption spectra (abs=log (1/int)). The absorption spectra were then normalised by standard normal variate (SNV) transformation to minimise spectral variations due to light scattering and height variations in the slices (Barnes, Dhanoa, & Lister, 1989).

The scanning was performed in an experimental pilot plant under conditions similar to industrial. The samples were run at random to suppress the influence of systematic, non-relevant spectral variation. The two faces of each slice and ROIs were scanned. The average spectrum from each face of each slice and ROI was calculated.

2.3 Reference analysis

After scanning, samples were minced and subjected to chemical analysis in triplicate. Water content was analysed by drying at 103 ± 2 ºC until reaching a constant weight (AOAC, 1990); the average standard deviation of triplicates was 0.21%. The total fat content was performed according to the AOAC (2006) method, using the Foss Soxcap 2047 system (hydrolysis step) in combination with soxtec extraction 2055 system (Foss Analytical, Denmark); the average standard deviation of triplicates was 0.79%. Chloride content was analysed according to ISO 1841-2 (1996) using a potentiometric titrator 785 DMP Titrino (Metrohm, Herisau,

Switzerland) and results were expressed as percentage of NaCl; the average standard deviation of triplicates was 0.03%.

2.4 Calibration and validation

The 37 hams were split into two sets, calibration (24 hams) and validation (13 hams). To ensure similar variation in composition in the calibration and validation sets, a stratified sampling method was performed. Three levels for salt and two levels for fat were considered to classify hams according to the combination of these levels. For those hams where different ROIS were used, the average composition of the ROIS was calculated. The water content was not considered because it was expected more variation for water between ROIS than between hams. Then hams were randomly sampled within each class, 2/3 of samples for the calibration set and 1/3 for the validation set. The calibration data set contained 82 average spectra (the spectra of two faces from 24 slices and 17 ROIs), whereas the validation data set contained 42 average spectra (the spectra of two faces from 13 slices and 8 ROIs).

Partial least squares regression (PLSR) was used for to develop calibration models between NIR data and reference values. The Q^2cum index from XLSTAT package (Addinsoft, Paris, France) was used to determine the number of PLS factors to use in the models. This index measures the global contribution of the *h* first PLS factors to the predictive quality of the model and is calculated as follows:

$$Q^2cum(h) = 1 - \prod_{j=1}^{h} \frac{\sum_{k=1}^{q} PRESS_{kj}}{\sum_{k=1}^{q} SE_{k(j-1)}}$$

The index involves the PRESS statistic (which requires a cross-validation), and the Sum of Squares of Errors (SSE) for a model with one less factor. The most stable model with low prediction error gives the maximum Q^2cum.

Multivariate correlation coefficient (R^2), the root mean square error of the model fitting (RMSE) and the residual predictive deviation (RPD) statistic were used to evaluate the models. RPD is the ratio between the standard deviation of the reference values and the error of the model. PLSR analyses were performed with XLSTAT.

The developed PLSR models for each component (water, fat and salt) were then applied to spectra of the validation data set and the root mean square error of prediction (RMSEP) and the RPD were calculated.

The models were also used to predict the composition in each pixel of the multi-spectral images to visualise the distribution of these components within the slice.

3. Results and discussion

3.1 Reference measurements

Table 1 shows the minimum, maximum, average and standard deviation of water, fat and salt contents in the calibration and validation data sets. The two sets had quite similar characteristics, as was intended in the splitting process of the data set. There was a wide range in concentrations of salt, water and fat contents which gave a good basis for modelling.

3.2 Spectral features of dry-cured ham samples

Figure 2 shows the average NIR absorbance spectra from the calibration samples. The spectra were rather smooth across the spectral region. The fat and water bands should, theoretically, appear around 930 nm and 970 nm respectively (Osborne & Fearn, 1986). The absorbance peak at around 970 nm is assigned to the O-H stretch second overtone in water, while the absorbance peak at 930 nm, which is too small to discern in the figure, corresponds to the third overtone C-H stretch in the methylene group of fat. Some details in the spectra are easier to see in the spectra after correction by the standard normal variate (SNV) pre-processing method. Although there was a trend toward samples with high fat content to show high values in the 900-940 nm band and a trend toward samples with high water contents to show high values in the 960-1000 nm, the shown spectra illustrate the complexity of the data. This is typical for NIR spectra from this spectral region; the main spectral components are strongly overlapped, the salt induces spectral shifts, and light scattering and colour can induce large offset variations. The use of multivariate modelling is a prerequisite to extract systematic and quantitative information.

3.3 Modelling of water, fat and salt contents in dry-cured ham slices by PLSR

The results of calibration for water, fat and salt are summarised in Figure 3.Water content was estimated with 7 PLS factors, an R^2 of 0.956 and RMSE of 1.03%. Fat content was estimated with 6 PLS factors, an R^2 of 0.921 and RMSE of 1.36%. Salt content was estimated with 8 PLS factors, an R^2 of 0.912 and RMSE of 0.54%. The estimated values with PLSR models

were unbiased in the whole range of reference values for the three components (water, fat and salt). The magnitude of the RMSE values obtained in this study will not permit the exact estimation of the composition of the product; however, it is high enough to classify the products into defined quality categories.

Figure 4 shows the regression coefficients of the PLSR models. It is often difficult to interpret regression coefficients for models consisting of as many as 6-8 PLS factors. Generally, wavelengths with high positive values are positively correlated with the dependent variable (water, fat or salt contents), negative values are negatively correlated, and values close to zero do not contribute much to explain the chemical variation. For fat there were high positive coefficients in the 900-940 nm range, which corresponds well with the absorption peak of C-H stretch. For water, a positive coefficient peak in the 960 – 1000 nm region was expected. However, there was a negative value at 980 nm. This negative value was probably due to the large variation in salt that induces a shift in the water peak. This shift has to be compensated for in the calibration and typically results in this kind of effect on the regression coefficient. These effects make it difficult to interpret the regression coefficients for water since the peaks are not fixed according to wavelength. It can be noted that the regression coefficients for salt was quite similar to those of water in the water peak region, but with the opposite sign.

3.4 Validation of PLSR models

The quality of the calibration models was evaluated by RMSEP and the RPD in the validation data set (Figure 5). The RPD values were 3.7, 3.6 and 2.5 for water, fat and salt, respectively. Conzen (2006) suggested that a good model for quality control should have an RPD > 5, but models with lower RPD values could still be used for screening purposes. The RMSEP and RPD for fat were 1.36% and 3.6 respectively, which were similar to the RMSE and RPD of calibration, indicating that the model was quite robust. Prevolnik et al. (2011) and Gaitán-Jurado et al. (2008) developed NIR predictive models with 7 PLS factors for fat content in minced ham and minced sausages respectively. They achieved lower RMSEP values: 0.43% in minced ham and 0.71% in minced sausages, because the samples were more homogeneous. However, the RMSEP of a model that used the average of 7 NIR spectra obtained at the surface of intact sausage slices was 1.47% (Gaitán-Jurado et al., 2008), similar to our results.

The RMSEP for water (1.34%) and salt (0.71%) were about 30% higher than the RMSE of calibration, indicating a possible overfitting in the calibration despite the fact that we used

Q^2cum index to select the number of PLS factors. The RMSEP for water in this study was lower than the RMSE of cross-validation (RMSECV) obtained by Collell et al. (2011) when measuring at the lean surface of whole hams during the processing (2.39% for hams after one month of processing and 3.51% for hams at the end of the process). Although they used higher spectra resolution and 16 PLS factors, their models had lower predictive ability than our NIR imaging system. This may have been in part due to the low penetration of the NIR device and the NIR point measurements of the surface used by Collell et al. (2011), which could have produced a less representative sampling of the ham.

In the case of salt prediction, the RMSECV obtained by Collell et al. (2011) when measuring at the surface of hams during processing were 0.43% for hams after one month of processing (model with 18 PLS factors) and 1.13% for hams at the end of the process (model with 10 PLS factors). The RMSEC of the latter model was lower than our RMSEP (0.71%) and similar to our error of model fitting (RMSE = 0.54%).

Nevertheless, the RPD value for water and salt were 3.7 and 2.5 respectively, which could be considered high enough for screening.

Figure 5 shows the predicted versus measured for water, fat and salt. As in the calibration, the predicted values were unbiased in the whole concentration range for the three components (water, fat and salt). There were small differences between the predicted values of the two surfaces from each sample. Consequently, RMSEP values hardly changed when the average of the spectra from the two surfaces of each sample was used for the prediction (RMSEP: 1.30 %, 1.31 % and 0.68 % for water, fat and salt, respectively). The NIR sampling from one side gave a good representation of the whole sample, suggesting that the slices were quite homogeneous throughout the sample thickness of 2.5 cm. If a larger variation between the two sides of the slices is encountered, then the average of the scans from each side would probably give better accuracy than the average of scans from one side.

3.5 Distributional images

Figures 6(a), 6(b) and 6(c) show the estimated 2D distribution of water, fat and salt in the same ham slice respectively. The average estimated values, based on single pixel predictions, for water, fat and salt contents in the this sample (43.92%, 11.60% and 7.79% respectively) were similar to the measured contents (43.53 %, 12.16% and 7.93% respectively). There was not a homogeneous distribution. Although part of the subcutaneous fat is usually removed

from the hams before deboning and pressing into a parallelepiped shape, part of it remained in the ham, as can be seen on the upper and lower left side of the fat image. Intermuscular fat can also be discerned in the centre of the image.

As was expected, the muscular tissue just below the subcutaneous fat dried slowly during drying and showed the highest water content. A gradient of water content from the right side to the left side in the water image can be seen.

In the predicted salt image, slightly higher salt content is observed in the central part of the ham slice, in concordance with the results showed using computed tomography by Santos-Garcés et al. (2012). Salt diffuses from external parts to internal parts of the ham during the first stages of the drying process and from internal parts to external parts during the last stages to achieve the same NaCl/water ratio in the whole ham. However, salt diffuses more rapid during the first stages of the drying process than during the last stages (Costa-Corredor, Pakowski, Lenczewski, & Gou, 2010), which can explain the higher predicted salt content in the internal zones of the ham.

The heterogeneous distribution of components within the slice confirms the importance of correct sampling when probing hams with NIR. Measurements in limited locations can give large deviations from the average values. NIR interactance imaging samples the whole surface, as well as in depth, and the prediction estimates are therefore less affected by the sample heterogeneity than the average of several NIR point measurements. Moreover, the image analysis can provide valuable information about the homogeneity of the sample, which could be used for process and quality control. For instance, the European quality label of the Traditional Speciality Guaranteed (TSG) *Jamon Serrano* defines, within the product specification, that the difference in water content between the internal part and the external part of the ham cannot be higher than 12%. Nowadays, a subsample of hams within each production batch is randomly selected and a 15 mm thick slice is sampled from each ham. This slice is divided into two parts (external and internal part) and chemical analyses are performed to check the TSG product specification.

4. Conclusions

NIR interactance hyperspectral imaging can be used for on-line prediction of the average water, fat and salt contents in packaged slices of dry-cured ham with sufficient accuracy for

screening purposes. It can also provide information about the spatial distribution of water, fat and salt within the slice.

5. Acknowledgements

This work was supported by the Sixth RTD Framework Programme Q-porkchains (Contract no. FOOD-CT-2007-036245) and the COST (Ref. COST Action FA1102). The information in this document reflects only the authors' views and the Community is not liable for any use that may be made of the information contained therein.

6. References

AOAC (1990). Official method 950.46, Moisture in meat, B. Air drying. In K. Helrich (Ed.) (15th ed.). *Official methods of analysis of the association of official analytical chemists* (Vol. II, pp. 931). Arlington: Association of Official Analytical Chemists, Inc.

AOAC (2006). Official method 991.36, fat (crude) in meat and meat products. Retrieved from: http://www.aoac.org/oma_revision/toc.htm.

Arnau, J., Guerrero, L., Casademont, G., & Gou, P. (1995). Physical and chemical changes in different zones of normal and PSE dry-cured ham during processing. *Food Chemistry*, *52 (1)*, 63-69.

Barnes, R. J., Dhanoa, M. S., & Lister, S. J. (1989). Standard Normal Variate Transformation and De-trending of Near-Infrared Diffuse Reflectance Spectra. *Applied Spectroscopy, 43(5)*, 772-777.

Blasco, A., Gou, P., Gispert, M., Estany, J., Soler, Q., & Diestre, A. (1994) Comparison of 5 types of pig crosses. 1. Growth and carcass traits. *Livestock Production Science*, *40 (2)*, 171-178.

Boadas, C., Gou, P., Valero, A., & Arnau, J. (2001). Changes in different zones of dry-cured ham during drying - Moisture and sodium chloride content. *Fleischwirtschaft*, *81 (1)*, 91-93.

Collell, C., Gou, P., Arnau, J., & Comaposada, J. (2011). Non-destructive estimation of moisture, water activity and NaCl at ham surface during resting and drying using NIR spectroscopy. *Food Chemistry*, *129 (2)*, 601-607.

Collell, C., Gou, P., Arnau, J., Munoz, I., & Comaposada, J. (2012). NIR technology for on-line determination of superficial a(w) and moisture content during the drying process of fermented sausages. *Food Chemistry*, *135 (3)*, 1750-1755.

Conzen, J. P. (2006). *Multivariate calibration, a practical guide for developing methods in the quantitative analytical chemistry*. Ettlingen,Germany: Bruker Optik GmbH.

Costa-Corredor, A., Muñoz, I., Arnau, J., & Gou, P. (2010). Ion uptakes and diffusivities in pork meat brine-salted with NaCl and K-lactate. *LWT-Food Science and Technology*, *43 (8)*, 1226-1233.

Costa-Corredor, A., Pakowki, Z., Lenczewski, T., & Gou, P. (2010). Simulation of simultaneous water and salt diffusion in fermented sausages by the Stefan-Maxwell equation. *Journal of Food Engineering, 97 (3),* 311-318.

Ellekjaer, M. R., Hildrum, K. I., Naes, T., & Isaksson T. (1993). Determination of the sodium chloride content of sausages by near infrared spectroscopy. *Journal of Near Infrared Spectroscopy, 1 (1)*, 65-75.

Gaitán-Jurado, A. J., Ortiz-Somovilla, V., España-España, F., Pérez-Aparicio, J., & De Pedro-Sanz, E. J. (2008). Quantitative analysis of pork dry-cured sausages to quality control by NIR spectroscopy. *Meat Science, 78 (4)*, 391-399.

Garcia-Gil, N., Santos-Garcés, E., Muñoz, I., Fulladosa, E., Arnau, J., & Gou, P. (2012). Salting, drying and sensory quality of dry-cured hams subjected to different presalting treatments: Skin trimming and pressing. *Meat Science, 90 (2)*, 386–392.

Gou, P., Guerrero, L., & Arnau, J. (1995) Sex and crossbreed effects on the characteristics of dry-cured ham. *Meat Science*, *40 (1)*, 21-31.

Guerrero, L., Gou, P., Alonso, P., & Arnau, J. (1996). Study of the Physicochemical and Sensorial Characteristics of Dry-Cured Hams in Three Pig Genetic Types. *Journal Science of Food and Agricultural*, *70 (4)*, 526-530.

Hersleth, M., Lengard, V., Verbeke, W., Guerrero, L., & Næs, T. (2011). Consumers' acceptance of innovations in dry-cured ham: Impact of reduced salt content, prolonged aging time and new origin. *Food Quality and Preference*, *22 (1)*, 31–41.

Hildrum, K. I., Nilsen, B. N., Westard, F., & Wahlgren, N. M. (2004). In-line analysis of ground beef using a diode array near infrared instrument on a conveyor belt. *Journal of Near Infrared Spectroscopy, 12 (6)*, 367-376.

Huang, H., Yu, H., Xu, H., & Ying, Y. (2008). Near infrared spectroscopy for on/in-line monitoring of quality in foods and beverages: A review. *Journal of Food Engineering, 87 (3)*, 303-313.

ISO 1841-2 (1996). Meat and meat products. *Determination of chloride content -Part 2: Potentiometric method (Reference method)*. Geneva: International Organization for Standardization.

Lebret, B. (2008). Effects of feeding and rearing systems on growth, carcass composition and meat quality in pigs. *Animal*, *2 (10)*, 1548-1558.

O'Farrell, M., Wold, J. P., Høy, M., Tschudi, J., & Schulerud, H. (2010). Online Fat Content Classification of Inhomogeneous Pork Trimmings Using Multispectral NIR Interactance Imaging. *Journal of Near Infrared Spectroscopy, 18 (2)*, 135-146.

Osborne, B. G., & Fearn, T. (1986). *Near infrared spectroscopy in food analysis*. Essex: Longman Scientific and Technical. UK.

Prevolnik, M., Škrlep, M., Janeš, L., Velikonja-Bolta, Š., Škorjanc, D., & Čandek-Potokar, M. (2011). Accuracy of near infrared spectroscopy for prediction of chemical composition, salt content and free amino acids in dry-cured ham. *Meat Science, 88 (2)*, 299-304.

Prieto, N., Roehe, R., Lavín, P., Batten, G., & Andrés, S. (2009). Application of near infrared reflectance spectroscopy to predict meat and meat products quality: A review. *Meat Science, 83 (2)*, 175-186.

Resano, H., Sanjuán, A. I., Cilla, I., Roncalés, P., & Albisu, L. M. (2012). Sensory attributes that drive consumer acceptability of dry-cured ham and convergence with trained sensory data. *Meat Science*, *84 (3)*, 344–351.

Santos-Garcés, E., Muñoz, I., Gou, P., Sala, X., & Fulladosa, E. (2012). Tools for Studying Dry-Cured Ham Processing by Using Computed Tomography. *Journal of Agricultural and Food Chemistry*, *60 (1)*, 241-249.

Segtnan, V. H., Høy, M., Lundby, F., Narum, B., & Wold, J. P. (2009). Fat distribution analysis in salmon fillets using non-contact near infrared interactance imaging: a sampling and calibration strategy. *Journal of Near Infrared Spectroscopy, 17 (5)*, 247-253.

Shackelford, S. D., Wheeler, T. L., & Koohmaraie, M. (2004). Development of optimal protocol for visible and near-infrared reflectance spectroscopic evaluation of meat quality. *Meat Science, 68 (3)*, 371-381.

Wold, J. P., Johansen, I. R., Haugholt, K. H., Tschudi, J., Thielemann, J., Segtnan, V. H., et al. (2006). Non-contact transflectance NIR imaging for representative on-line sampling of dried salted coalfish (bacalao). *Journal of Near Infrared Spectroscopy, 14 (1)*, 59-66.

Wold, J. P., O'Farrell, M., Høy, M., & Tschudi, J. (2011). On-line determination and control of fat content in batches of beef trimmings by NIR imaging spectroscopy. *Meat Science, 89 (3)*, 317–324.

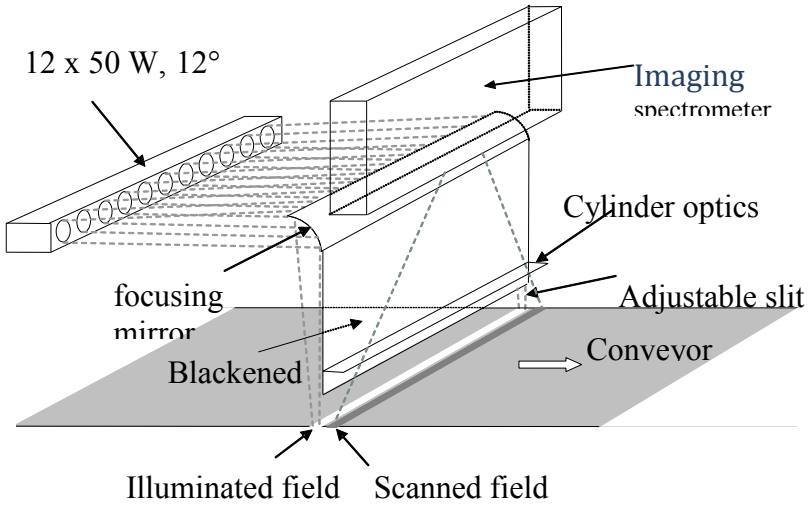

Figure 1. Principle drawing of on-line NIR non-contact interactance imaging system.

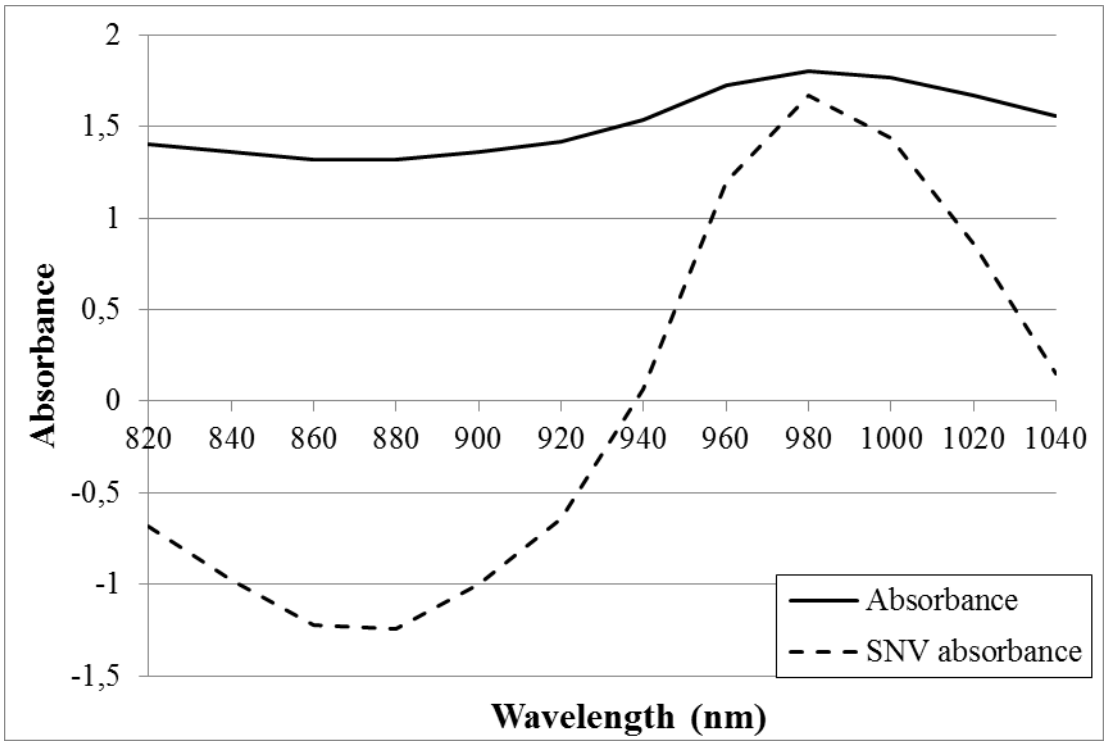

Figure 2. Average NIR interactance absorbance spectra from the calibration set of samples and the same spectra after correcting by the standard normal variate (SNV) pre-processing method.

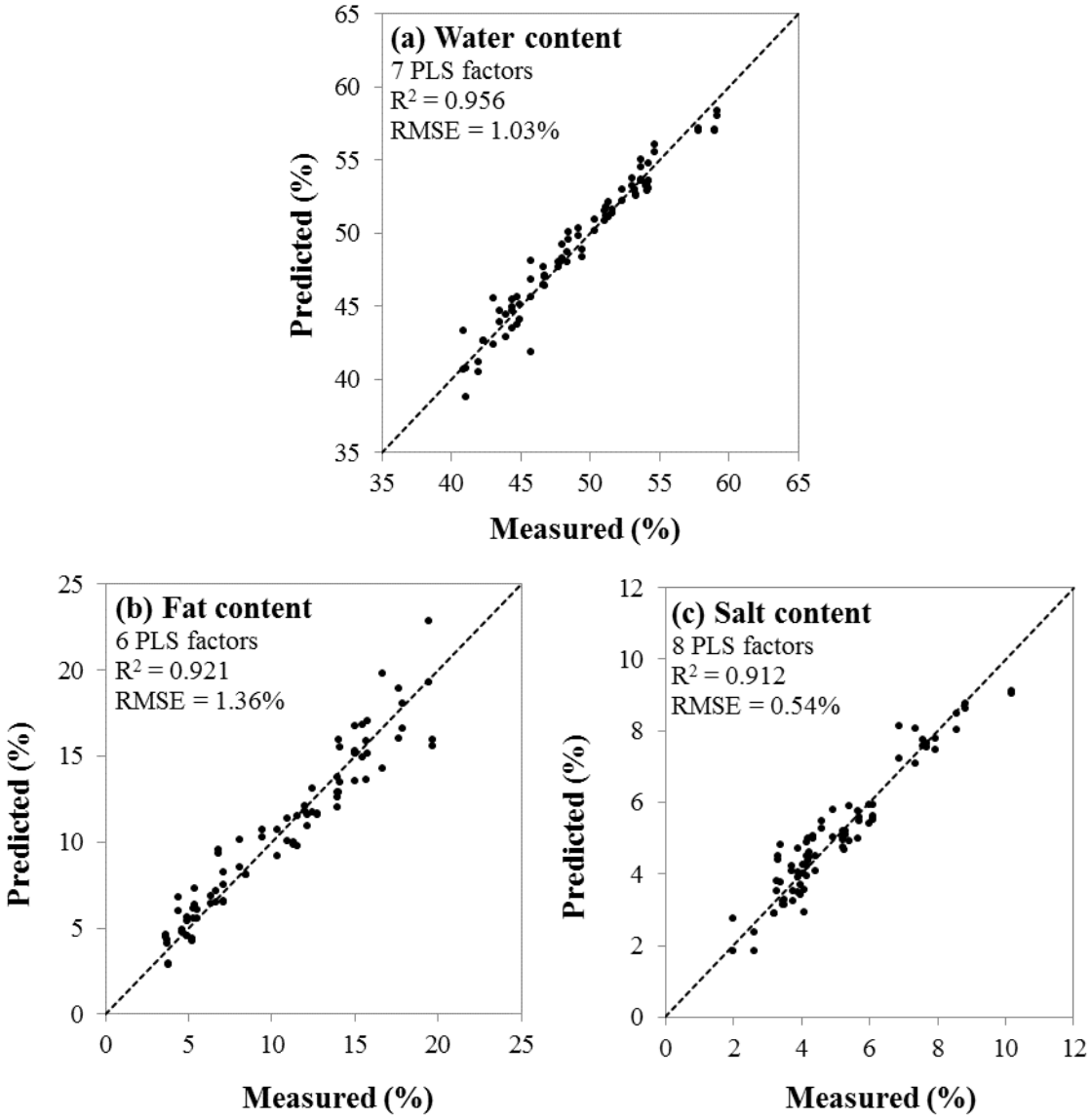

Figure 3. Relationship between the predicted and the measured water (a), fat (b) and salt (c) contents for the calibration data set (including the prediction of the two faces of each sample). The line represents the perfect 1:1 relationship between x and y.

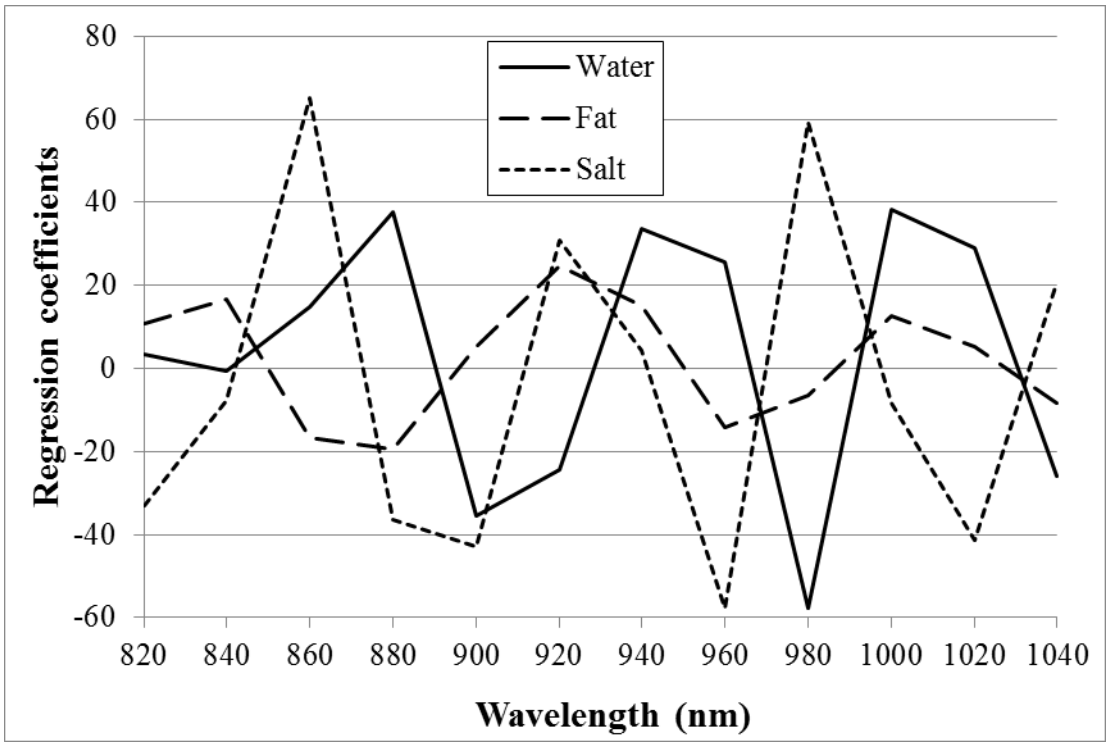

Figure 4. Regression coefficients of each wavelength for predictive models for water, fat and salt content.

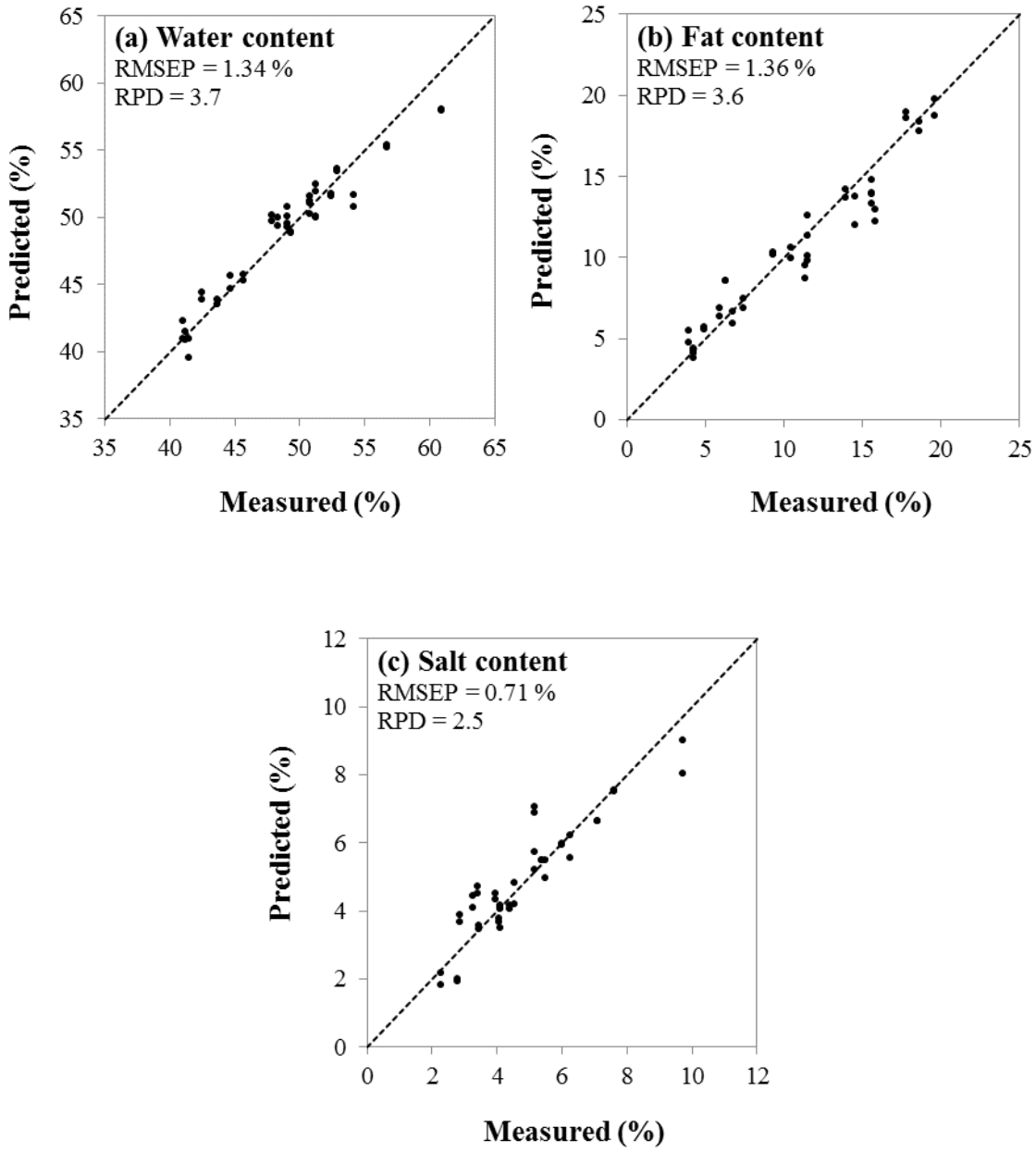

Figure 5. Relationship between the predicted and the measured water (a), fat (b) and salt (c) contents for the validation data set (n = 41). The line represents the perfect 1:1 relationship between x and y.

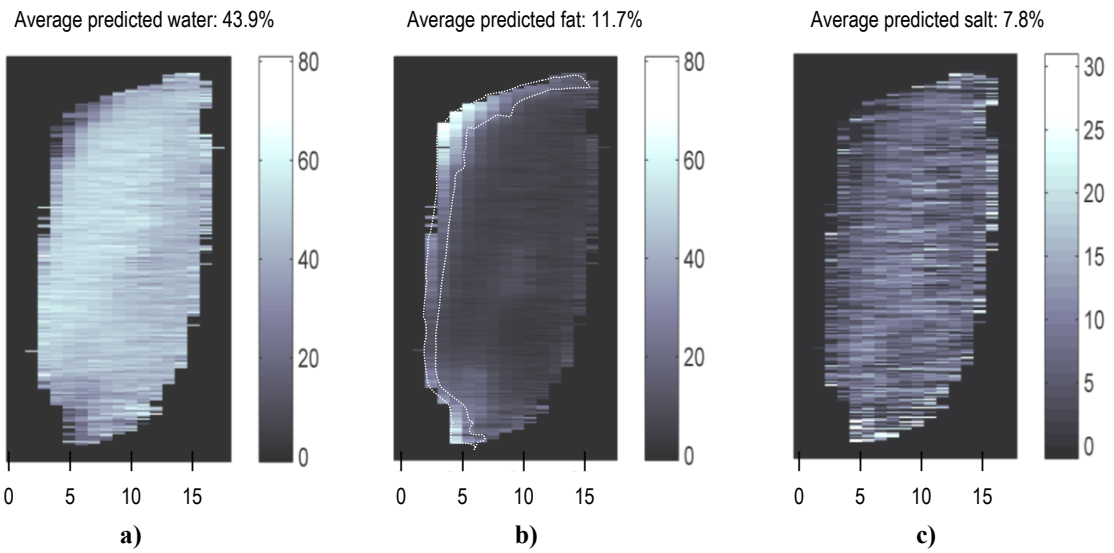

Figure 6. 2D distribution within one slice of ham for water (a), fat (b) and salt (c) contents. Average predicted values are based on single pixel predictions. The bars to the right of each image are grey scales indicating per cent concentration at pixel level. The horizontal axis on each image indicates scale in cm. The dotted line on the fat image indicates the area of subcutaneous fat layer.